

Quantum State Preparation with Optimal Circuit Depth: Implementations and Applications

Xiao-Ming Zhang,¹ Tongyang Li,¹ and Xiao Yuan^{1,*}

¹Center on Frontiers of Computing Studies, Peking University, Beijing 100871, China

Quantum state preparation is an important subroutine for quantum computing. We show that any n -qubit quantum state can be prepared with a $\Theta(n)$ -depth circuit using only single- and two-qubit gates, although with a cost of an exponential amount of ancillary qubits. On the other hand, for sparse quantum states with $d \geq 2$ non-zero entries, we can reduce the circuit depth to $\Theta(\log(nd))$ with $O(nd \log d)$ ancillary qubits. The algorithm for sparse states is exponentially faster than best-known results and the number of ancillary qubits is nearly optimal and only increases polynomially with the system size. We discuss applications of the results in different quantum computing tasks, such as Hamiltonian simulation, solving linear systems of equations, and realizing quantum random access memories, and find cases with exponential reductions of the circuit depth for all these three tasks. In particular, using our algorithm, we find a family of linear system solving problems enjoying exponential speedups, even compared to the best-known quantum and classical dequantization algorithms.

The speed limit of quantum state preparation is a question with fundamental and practical interests, determining the efficiency of inputting classical data into a quantum computer, and playing as a critical subroutine for many quantum algorithms, such as in machine learning [1–3] and Hamiltonian simulations [4, 5]. Without ancillary qubit, an exponential circuit depth is inevitable to prepare an arbitrary quantum state [6–16] and the optimal result $\Theta(2^n/n)$ is recently obtained by Sun *et al.* [17]. Leveraging ancillary qubits, the circuit depth could be reduced to be sub-exponential scaling [17–20], yet in the worse case with an exponential number of ancillas. Very recently, the optimal circuit depth $\Theta(n)$ was achieved by [17, 20] with $O(2^n)$ [17] and $\tilde{O}(2^n)$ [20] ancillary qubits.

Despite the previous results in minimizing circuit depth, the sub-exponential circuit depth is only achieved at the cost of exponential space complexity. Therefore, it is challenging to implement those state preparation protocols in the noisy intermediate-scale quantum or early fault-tolerant quantum regime when the number of qubits is limited. Moreover, when considering applications in the field of quantum machine learning, strong data structure assumptions leave space for quantum-inspired classical algorithms. With a classical data structure enabling l^2 sampling, there are classical algorithms with poly-logarithmic runtime dequantizing the quantum algorithms for recommendation systems [21], solving linear systems [22, 23], semidefinite programs [24], etc. These results show that space resources should not be neglected when discussing the quantum exponential advantages.

In practice, the data may behave with a certain structure. Indeed, if the one imposes certain restrictions on the target quantum states, the circuit depth and the ancillary qubit number might be further reduced [25–30]. A typical scenario that has both theoretical and practical relevance is the sparse data structure, such as sparse classical data, Hamiltonians of physics systems, etc. Using a constant number of ancillary qubits, arbitrary d -sparse quantum states (with d non-zero entries) can be prepared using a circuit depth of $O(dn)$ [25–28]. However, it was unclear if the sparse preparation procedure could be further sped up with more (polynomial with n) ancillary qubits. The fundamental speed limit of sparse state preparation is still an open question, which is important for

studying the ultimate power of quantum machine learning algorithms.

In this work, we study the speed limit of quantum state preparation. We first develop a deterministic algorithm (independent of Refs. [17, 20]) for preparing an arbitrary quantum state with optimal circuit depth $\Theta(n)$ and $O(2^n)$ ancillary qubits. We next develop an algorithm for d -sparse quantum states ($d \geq 2$) that achieves the optimal circuit depth $\Theta(\log(nd))$, exponentially faster than the best-known results [25–27]. The sparse state preparation requires $O(nd \log d)$ ancillary qubits, which is also nearly optimal. Based on the results, we find a family of linear system tasks that can be solved with the circuit depth and the number of ancillary qubits being $O(\text{poly}(n))$, and hence show an exponential speedup compared to the best known quantum and classical dequantization algorithms. We also show how our techniques can be applied to improving Hamiltonian simulations and QRAMs.

Quantum state preparation.— We first introduce our algorithm for preparing an arbitrary n -qubit quantum state. The target state can be expressed as

$$|\psi\rangle = \sum_{k=0}^{N-1} a_k |k\rangle, \quad (1)$$

with $N = 2^n$, $a_i \in \mathbb{C}$, $\sum_{k=0}^{N-1} |a_k|^2 = 1$, and $|k\rangle \equiv |k_n k_{n-1} \dots k_1\rangle$ being the basis with bits k_j for $j = 1, 2, \dots, n$. Without loss of generality, the task of quantum state preparation is to prepare $|\psi\rangle$ from an initial product state $|0\rangle^{\otimes n}$ using single- and two-qubit gates. We have the following result.

Theorem 1 (Arbitrary quantum state preparation). *With only single- and two-qubit gates, an arbitrary n -qubit quantum state can be deterministically prepared with a circuit depth $\Theta(n)$ and $O(N)$ ancillary qubits.*

Our method saturates the circuit depth lower bound $\Omega(n)$ [17, 18]. Below we sketch our protocol with five stages and refer to [31] for the formal description.

At stage 1, we introduce an $(n+1)$ -layer binary tree, H , composed of qubits [Fig. 1(a)]. Layer l ($0 \geq l \geq n$) of the tree is denoted as H_l . Initially, the root of H is initialized as

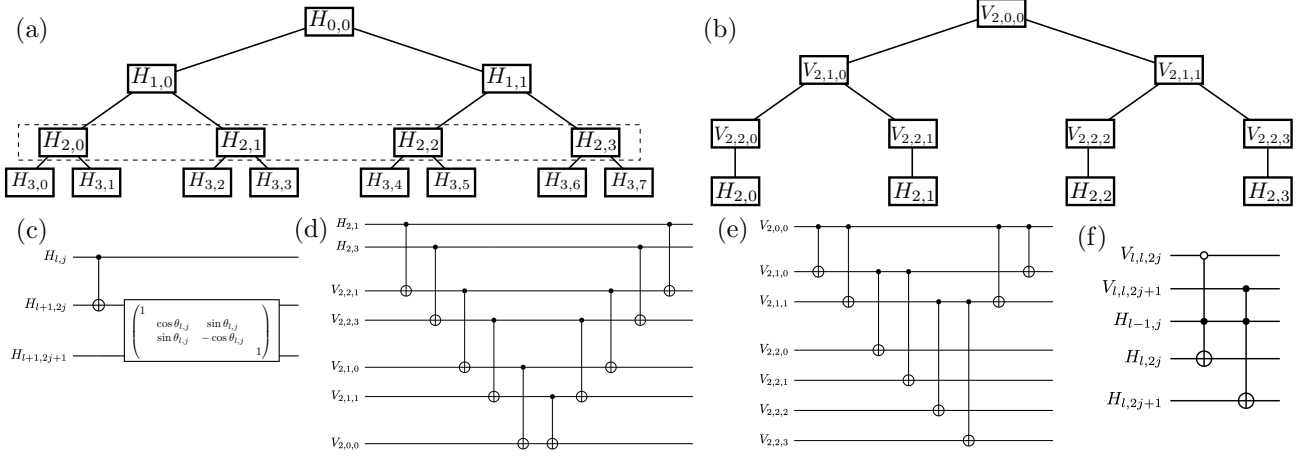


FIG. 1: Sketch of optimal arbitrary quantum state preparation. (a) Architecture of the binary tree H . (b) Architecture of the binary tree V_2 connected to H_2 . Here, $V_{2,\text{root}}$ is $V_{2,2,0}$ and $V_{2,\text{leaf}}$ is the layer containing $V_{2,2,j}$. (c) Quantum circuit for partial fanout at stage 1. Operations for the same l and different j are implemented in parallel. (d) Quantum circuit for transformation $|(k, 2)\rangle_{H_2}|0\rangle_{V_{2,\text{root}}} \rightarrow |(k, 2)\rangle_{H_2}|k_2\rangle_{V_{2,\text{root}}}$ at stage 2. (e) Quantum circuit for transformation $|k_2\rangle_{V_{2,\text{root}}}|0\rangle_{V_{2,\text{leaf}}}^{\otimes 4} \rightarrow |k_2\rangle_{V_{2,\text{root}}}|k_2\rangle_{V_{2,\text{leaf}}}^{\otimes 4}$ at stage 3. (f) Quantum circuit for uncomputation operations at stage 4. Operations for the same l and different j are implemented in parallel.

$|1\rangle$ while all other qubits are initialized to $|0\rangle$. We perform *partial fanout* [Fig. 1(c)] (with parameters determined by the coefficients a_k of the target state $|\psi\rangle$) layer-by-layer from the root of H . At the l th step, if a node at H_{l-1} is at state $|1\rangle$, we flip one of its children in a superposition way. After n steps, each layer of H has exactly one excitation (qubit at state $|1\rangle$), and the parent of an excitation is also an excitation. Following by one layer of single qubit phase gates on all leaves, the quantum state of H can be prepared as an isometry of Eq. (1)

$$\sum_{k=0}^{2^n-1} a_k |1\rangle_{H_0} \bigotimes_{l=1}^n |(k, l)\rangle'_{H_l}, \quad (2)$$

where $|1\rangle_{H_0}$ corresponds to the root node, and $\bigotimes_{l=1}^n |(k, l)\rangle'_{H_l}$ corresponds to state at the l th layer. Here $|(k, l)\rangle' \equiv |0\rangle^{\otimes(k,l)}|1\rangle|0\rangle^{\otimes 2^l-(k,l)-1}$ represents the state such that the excitation at the l th layer is the (k, l) th qubit at this layer, and $(k, l) \equiv k_n k_{n-1} \cdots k_{n-l+1}$ represents the last l digits of k . The partial fanout for each layer have circuit depth $O(1)$, so the circuit depth of this stage is $O(n)$.

At stage 2, for each l , we introduce another l -layer binary tree V_l with its leaves connecting to H_l [Fig. 1(b)]. Denoting the root of V_l as $V_{l,\text{root}}$, we aim at performing the mapping $|(k, l)\rangle'_{H_l}|0\rangle_{V_{l,\text{root}}} \rightarrow |(k, l)\rangle'_{H_l}|k_{n-l+1}\rangle_{V_{l,\text{root}}}$ with k_l being the l th digit of the binary string k . One of the trick is that (k, l) and k_{n-l+1} have the same parity, so we just need to flip $V_{l,\text{root}}$ when (k, l) is odd. This can be realized with $O(l)$ layers of CNOT gates applied to V_l and H_l [Fig. 1(d)]. For each l , the transformation can be implemented in parallel. So with a total

circuit depth $O(n)$, we obtain

$$\sum_{k=0}^{2^n-1} a_k |1\rangle_{H_0} \bigotimes_{l=1}^n |(k, l)\rangle'_{H_l} |k_{n-l+1}\rangle_{V_{l,\text{root}}}. \quad (3)$$

The remaining task is to uncompute H . Let $H_{l,j}$ be the j th qubit at layer l , it can be observed that $H_{l,j}$ is at state $|1\rangle$, if and only if its parent is at state $|1\rangle$ and j has the same parity of k_{n-l+1} . Therefore, by flipping $H_{l,j}$ conditioned on the states of its parent and $V_{l,0}$, one can bring $H_{l,j}$ back to state $|0\rangle$. We expect to uncompute all nodes at layer H_l in a parallel way, so we need 2^l ‘‘copies’’ of $|k_{n-l+1}\rangle$. Based on the idea above, the uncomputation is realized in the following way.

At stage 3, we fanout the state of $V_{l,\text{root}}$ to $V_{l,\text{leaf}}$ (the leaf layer of V_l) in the form $|k_{n-l+1}\rangle_{V_{l,\text{root}}}|0\rangle_{V_{l,\text{leaf}}}^{\otimes 2^l} \rightarrow |k_{n-l+1}\rangle_{V_{l,0}}|k_{n-l+1}\rangle_{V_{l,\text{leaf}}}^{\otimes 2^l}$ with a circuit illustrated in Fig. 1(e). Each fanout takes a circuit depth $O(l)$ and the fanout for each l can be operated in parallel, so the total circuit depth is $O(n)$.

At stage 4, we uncompute H layer-by-layer from H_n to H_1 . When uncomputing the l th layer, the j th leaves at state $|k_l\rangle$ is used for uncompute $H_{l,j}$, and each parent qubit is used twice to uncompute two of its children [Fig. 1(f)]. Therefore, the uncomputation of each H_l has circuit depth $O(1)$, and the entire H is uncomputed with circuit depth $O(n)$.

At stage 5, we implement the fanout operation at stage 3 again, which uncompute $V_{l,\text{leaf}}$ for all l . In this way, all nodes except for $V_{l,\text{root}}$ are uncomputed and the quantum state becomes $\sum_{k=0}^{2^n-1} a_k \bigotimes_{l=1}^n |k_{n-l+1}\rangle_{V_{l,\text{root}}}$. Because $|k\rangle \equiv |k_n k_{n-1}, \dots, k_1\rangle$, the target state in Eq. (1) is obtained.

To summarize, the protocol works by first preparing a state that is isometric to Eq. (1) at stage 1 and then realize the inverse isometry by uncomputing the ancillary qubits in the other four stages. The protocol successfully achieves the optimal circuit

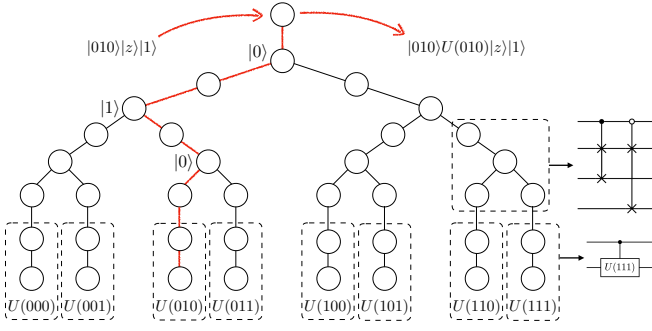


FIG. 2: Sketch of PUM for word register with single qubits. An example is given for index register at state $|010\rangle$. Each routing operation is realized with two controlled swap gates.

depth by utilizing the binary trees H and V_l , which is crucial for realizing parallel uncomputation.

Sparse quantum state preparation.— The protocol can be further improved if the target states are sparse. We first introduce two data structures that are useful for sparse state preparation and also many other applications as will be introduced later.

The first type is the product unitary selector. We define an n -word product unitary function $\hat{U}(k) \equiv \bigotimes_{l=1}^n \hat{U}_l(k)$, with $\hat{U}_l(k) \in \text{SU}(2)$, $k \in \{0, 1, \dots, d\}$. We define the selector unitary of \hat{U} as $\text{select}(\hat{U})$, which satisfies $\text{select}(\hat{U})|k\rangle|z\rangle = |k\rangle\hat{U}(k)|z\rangle$. Here, $|k\rangle$ is the basis of the $\lceil \log_2 d \rceil$ -qubits *index register*, and $|z\rangle$ is the basis of the n -qubits *word register*. Alternatively, it can be represented as

$$\text{select}(\hat{U}) \equiv \sum_{k=0}^{d-1} |k\rangle\langle k| \otimes \hat{U}(k). \quad (4)$$

We call a data structure performing Eq. (4) as the product unitary memory (PUM). We have the following result.

Lemma 1 (PUM). *Given an arbitrary $\lceil \log_2 d \rceil$ -index, n -word product unitary function $\hat{U}(k)$, $\text{select}(\hat{U})$ in Eq. (4) can be realized with circuit depth $O(\log(nd))$ and $O(nd)$ ancillary qubits using only single- and two-qubit gates.*

For $n = 1$, our PUM contains a binary tree of quantum routers and N memory cells. Each memory cell has a single-qubit oracle holder and pointer holder, and stores classically a single qubit gate $U(k)$. The protocol starts with a pointer qubit at state $|1\rangle$, and routing the state of word register and the pointer qubit into one of the memory cells with a path determined by the state of index register. Then, we apply controlled- $U(k)$ on each memory cell performing the transformation $|z\rangle|1\rangle \rightarrow U(k)|z\rangle|1\rangle$. By performing the inverse of the routing step, state $U(k)|z\rangle|1\rangle$ are routed back to the word register and pointer qubit. An example of PUM is given in Fig. 2. More details of PUM and the generalization to $n > 1$ are provided in Sec. III of [31].

The second type of oracles is for sparse Boolean functions. We consider an n -index, \tilde{n} -word Boolean function

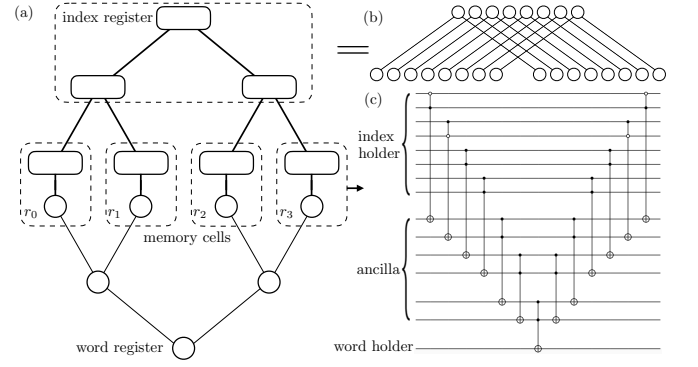


FIG. 3: Sketch of SBM for word register with single qubit. (a) Overall architecture. (b) The first and second layer of binary trees connecting index qubits. (c) The n -Toffoli gate stored in memory cell with $r_3 = 01101111$. It corresponds to $f(r_3) = f(01101111) = 1$.

$f : \{0, 1\}^n \rightarrow \{0, 1\}^{\tilde{n}}$. Let $\mathcal{S}_f = \{k | f(k) \neq 0 \dots 0\}$ containing all input indexes with non-zero output. We say that f is s -sparse if $|\mathcal{S}_f| \leq s$. Its corresponding sparse Boolean function selector satisfies $\text{select}(f)|k\rangle|z\rangle = |k\rangle|z \oplus f(k)\rangle$, where \oplus represents bit-wise XOR. Let $f_l(k)$ be the l th digit of $f(k)$, $\text{select}(f)$ can be expressed as a unitary

$$\text{select}(f) \equiv \sum_{k=0}^{2^n-1} |k\rangle\langle k| \bigotimes_{l=1}^{\tilde{n}} \left(f_l(k) \hat{X} + \bar{f}_l(k) \hat{1}_1 \right), \quad (5)$$

where $\bar{f}_l(k)$ is the NOT of $f_l(k)$, \hat{X} is the Pauli- X operator and $\hat{1}_m$ represents the m -qubit identity. We call a data structure performing Eq. (5) the sparse Boolean memory (SBM), and obtain the following result.

Lemma 2 (SBM). *Given an arbitrary n -index, \tilde{n} -word, s -sparse Boolean function f , $\text{select}(f)$ in Eq. (5) can be queried with circuit depth $O(\log(ns\tilde{n}))$ and $O(ns\tilde{n})$ ancillary qubits using only single- and two-qubit gates.*

For $\tilde{n} = 1$, the SBM contains s memory cells. Each memory cell has an n -qubit index holder, a single-qubit word holder, and stores one of the indexes r_w satisfying $f(r_w) = 1$. Each qubit at index register is connected to all memory cells with a binary tree. We first fanout the state of index register to the index holder of each memory cell using these binary trees [Fig. 3(a),(b)]. Then, at each memory cell, we perform n -Toffoli gates with the word holder as target qubit, conditioned on index holder at state $|r_w\rangle$. This performs the transformation $|k\rangle|0\rangle \rightarrow |k\rangle|k = r_w\rangle$. Note that with $O(n)$ ancillary qubits, n -Toffoli gates can be realized with circuit depth $O(\log n)$ [32]. We then apply a ‘‘parallel CNOT’’ gate with word register as target qubit and all word holders as controlled qubits. It can be realized with $O(\log s)$ circuit depth and performs the transformation $|z\rangle \rightarrow |z \bigoplus_{w=0}^{s-1} (k = r_w)\rangle = |z \oplus f(k)\rangle$ on the word register. Finally, the memory cells are uncomputed by applying n -Toffoli gates and index fanout operations again. In this way, we obtain the transformation in Eq. (5). Details of PUM and the generalization to $\tilde{n} > 1$ are provided in Sec. III

of [31].

Based on Lemma 1 and 2, we are now ready for our sparse state preparation protocol. Consider a d -sparse quantum state $\sum_{k=0}^{d-1} \psi_k |q_k\rangle$, where q_k is the index (with n digits) of the k th nonzero entries, we have the following result.

Theorem 2 (Sparse state preparation). *With only single- and two-qubit gates, arbitrary n -qubit, d -sparse ($d \geq 2$) quantum states can be deterministically prepared with a circuit depth $\Theta(\log(nd))$ and $O(nd \log d)$ ancillary qubits.*

As we prove in Lemma 3 of [31] that the circuit depth is lower bounded by $\Omega(\log(nd))$, our protocol also achieves the optimal circuit depth for sparse states. Below, we show how the protocol works. We introduce two registers A and B , consisting of $\tilde{n} = \lceil \log_2 d \rceil$ and n qubits, respectively, and initialized to $|0\rangle$. Then we prepare register A to state $\sum_{k=0}^{d-1} \psi_k |k\rangle_A$ using the non-sparse preparation method introduced in Theorem 1, which takes circuit depth $O(\log d)$ and space complexity $O(d)$. Next, we introduce an n -word product unitary function $\hat{U}_{\text{prep}}(k) = \bigotimes_{j=0}^{n-1} (q_{k,j} \hat{X} + \bar{q}_{k,j} \hat{I}_1)$, where $q_{k,j}$ is the j th digit of q_k . We query $\text{select}(\hat{U}_{\text{prep}})$ with register A as index register and register B as word register, and the output state is $\sum_{k=0}^{d-1} \psi_k |k\rangle_A |q_k\rangle_B$. According to Lemma 1, this step can be realized with circuit depth $O(\log(nd))$ and $O(nd)$ ancillary qubits. The remaining procedure is to uncompute register A . To do so, we introduce another n -index, \tilde{n} -word Boolean function f_{prep} . Let Q be a set containing all non-zero entries q_k of the target state. The definition of f_{prep} is that $f_{\text{prep}}(q_k) = k$ for $q_k \in Q$ and $f_{\text{prep}}(q) = 0$ for $q \notin Q$ (i.e. $\mathcal{S}_{f_{\text{prep}}} = Q$). We query $\text{select}(f_{\text{prep}})$ with register B as index register and register A as word register, and the state then becomes $\sum_{k=0}^{d-1} \psi_k |0\rangle_A |q_k\rangle_B$. The target state is obtained by tracing out register A . Because f_{prep} is d -sparse, according to Lemma 2, this step has circuit depth $O(\log(nd))$ and space complexity $O(nd \log d)$. So the total circuit depth and space complexity of sparse state preparation is $\Theta(\log(nd))$ and $O(nd \log d)$.

We next discuss applications of the results.

Hamiltonian simulation.— A Hamiltonian \hat{H} can generally be expressed as a linear combination of products of single qubit unitaries (such as Pauli strings)

$$\hat{H} = \sum_{p=0}^{P-1} \alpha_p \hat{V}(p), \quad (6)$$

for some $\alpha_p > 0$, $\hat{V}(p) = \bigotimes_{l=0}^{n-1} \hat{V}_l(p)$ and $\hat{V}_l(p) \in \text{SU}(2)$. Several advanced techniques, such as Taylor expansion [33] and qubitization [5], have been introduced to simulate the time evolution operator $e^{-i\hat{H}t}$ with optimal complexity with respect to the simulation accuracy. However, these advanced methods generally assume block-encodings [5, 34] (or standard-form encoding) as an important subroutine. We say that \hat{U} is a block-encoding [34] of \hat{H} if $(\langle 0|^{\otimes a} \otimes \mathbb{I}_n) \hat{U} (|0\rangle^{\otimes a} \otimes \mathbb{I}_n) \propto \hat{H}$ for some integer a . One common construction way of block-encoding is based on linear combination of unitaries [5]. We define \hat{G} as a quantum state preparation operator satisfying

$\hat{G}|0\rangle = |G\rangle \equiv \sum_p \sqrt{\alpha_p/\alpha} |p\rangle$ with $\alpha \equiv \sum_p \alpha_p$. It can be verified that $(\hat{G}^\dagger \otimes \mathbb{I}_n) \text{select}(\hat{V})(\hat{G} \otimes \mathbb{I}_n)$ is a block-encoding of \hat{H} . Conventional ways to implement $\text{select}(\hat{V})$ requires a circuit depth $O(nP)$, and the total circuit depth also increases linearly with n and P [4].

In contrast, according to Theorem 1 and Lemma 1, \hat{G}, \hat{G}^\dagger can be realized with circuit depth $O(\log P)$, and $\text{select}(\hat{V})$ can be realized with circuit depth $O(\log(Pn))$. So the block-encoding can be constructed with circuit depth $O(\log(nP))$. Combining qubitization [5] with our fast construction of block-encoding, we have the following result (see Sec. IV of [31] for details), which decreases the circuit depth exponentially to nP .

Theorem 3 (Hamiltonian simulation by qubitization). *Let \hat{H} be a Hermitian operator expressed as Eq. (6). Using only single- and two-qubit gates, the evolution $e^{-i\hat{H}t}$ can be simulated to error ε with circuit depth $O(\log(nP)(\alpha t + \log(1/\varepsilon)))$ and $O(nP)$ qubits.*

We note that another version of parallel Hamiltonian simulation has been proposed in Ref. [19], achieving doubly logarithmic circuit depth with respect to the precision $O(\log^3 \log(1/\varepsilon))$. The algorithm is based on quantum walk and uses a state preparation method with cubic circuit depth. In [31], we show that the circuit depth can be further reduced to $O(\log^2 \log(1/\varepsilon))$ using our state preparation method with linear circuit depth.

Solving linear systems.— Given a matrix $H \in R^{2^n \times 2^n}$ and vector $b \in R^{2^n}$, quantum algorithms of linear systems aim at generating an approximation of quantum state $|x\rangle$ proportional to $H^{-1} \cdot b$. For sparse, invertible H , $|x\rangle$ can be obtained with a circuit depth $O(\text{poly}(n))$ [1, 34, 35]. The results has also been generalized to non-sparse cases [36]. However, these quantum algorithms assume the query of quantum state preparation and Hamiltonian simulation oracles. In general, to achieve poly-logarithmic circuit depth, data structure with space complexity $O(2^n)$ is required, leaving rooms for classical dequantization algorithms [21–23]. Specifically, based on an analog data structure with $O(\text{nnz}(H) \cdot n)$ space complexity ($\text{nnz}(\cdot)$ refers to the number of non-zero entries), classical dequantization algorithms [22, 23] can sample from the distribution of the measurement outcomes of $|x\rangle$ with a circuit depth $O(\text{poly}(n))$.

Therefore, whether we could more efficiently solve linear systems heavily relies on efficiency of the quantum state preparation and Hamiltonian simulation oracles. Here, considering sparse matrices of Eq. (6), we show an exponential advantage of quantum computing algorithms. The main idea is to apply our sparse state preparation protocol as well as the Hamiltonian simulation algorithm for \hat{H} in the algorithm proposed in Ref. [35]. We therefore obtain the following result.

Theorem 4 (Solving linear system). *Let \hat{H} be a Hermitian expressed as Eq. (6) with condition number κ . Let $|b\rangle$ be a $O(\text{poly}(n))$ -sparse quantum state. With only single- and two-qubit gates, the quantum state $|x\rangle$ proportional to $H^{-1}|b\rangle$ can be approximately prepared to error ε using $\tilde{O}(\text{poly}(\log(nP), \alpha, \kappa))$ circuit depth and $O(\text{poly}(n, P))$*

qubits, where \tilde{O} neglects the logarithmic dependence on $\kappa, 1/\varepsilon$.

With $P, \alpha = O(\text{poly}(n))$, our method has $\tilde{O}(\text{poly}(n, \kappa))$ circuit depth and $O(\text{poly}(n))$ space complexity. In comparison, the data structures by classical dequantization algorithms [22, 23] have $O(\text{nnz}(\hat{H}) \log N) = O(NPn)$ space complexities, which is exponentially larger. Furthermore, assuming that $P, \alpha = O(1)$ and $|b\rangle$ is $O(1)$ -sparse, the circuit depth of our parallel method is further reduced to $\tilde{O}(\log(n)\text{poly}(\kappa))$, which is also exponentially lower than the depth $\tilde{O}(n\text{poly}(\kappa))$ of best-known quantum algorithms using sequential $\text{select}(\hat{H})$ [4, 33]; Yet, both of them have $O(n)$ space complexity. More details are provided in Sec. VI of [31].

QRAMs.— At last, we show applications of the results for realizing sparse QRAMs. Given a binary dataset $\mathcal{D} \equiv \{|D_k\rangle\}_{k=0}^{2^n-1} \in \{|0\rangle, |1\rangle\}^n$, QRAMs are memory architectures enabling the transformation

$$\text{QRAM}(\mathcal{D}) \sum_{k=0}^{2^n-1} \psi_k |k\rangle |0\rangle = \sum_{k=0}^{2^n-1} \psi_k |k\rangle |D_k\rangle. \quad (7)$$

Efficient implementation of QRAM is important for many applications, especially for quantum machine learning [37]. The conventional bucket-brigade QRAM architecture performs the transformation with $O(n)$ circuit depth using $O(N)$ ancillary qubits [38, 39]. If \mathcal{D} is d -sparse (with at most d non-zero elements), the space complexity can be significantly reduced using quantum read-only access memory (QROM) [40]. Alternatively, Eq. (7) can be realized by performing n -Toffoli gates for d times. However, these methods have circuit depth linear with d , which is not yet optimal.

On the other hand, by defining $f_{\text{qram}}(k) \equiv D_k$, Eq. (7) can be satisfied by $\text{select}(f_{\text{qram}})$. According to Lemma 2, we can obtain the following result.

Theorem 5 (Sparse QRAM). *With only single- and two-qubit gates, arbitrary QRAM(\mathcal{D}) in Eq. (7) with d -sparse \mathcal{D} can be implemented with circuit depth $O(\log(nd))$ and $O(nd)$ ancillary qubits.*

Our protocol thus has an exponentially lower circuit depth compared to existing ones [38, 40], while the space complexity remains polynomial.

Moreover, we can also construct a generalized QRAM for continuous amplitude, i.e. $|D_k\rangle \in \mathbb{C}^2$, based on PUM in Lemma 1. Our method has query circuit depth $O(n)$ and $O(N)$ ancillary qubits that are independent on the precision ε (see Sec. VI of [31] for details). In comparison, the naive method based on digitizing D_k has circuit depth $O(n \log 1/\varepsilon)$ and $O(N + \log 1/\varepsilon)$ ancillary qubits.

Discussions.— For arbitrary quantum state preparation, we have proposed algorithms with an optimal circuit depth $\Theta(n)$ and $O(N)$ ancillary qubits. For d -sparse ($d \geq 2$) quantum states, we can achieve the optimal circuit depth $\Theta(\log(nd))$ with $O(nd \log d)$ ancillary qubits. While Theorem 1, 2 assume that only single- and two-qubit gates are allowed, our results can be generalized to elementary gates operations

applied to constant number of qubits. There are several interesting future directions. The first is to find the optimal space-time trade-off for sparse state preparation. The second is to explore the relationship between the complexity of decomposing a given target state and properties of the target states, such as sparsity and entanglement [30]. We also show that for sparse matrices of Eq. (6), the Hamiltonian simulation and linear systems can be solved with poly-logarithmic circuit depth with a number of ancillary qubits proportional to the system size. It is also interesting to generalize our method to other quantum machine learning algorithms [2, 3], and explore the practical applications.

Acknowledgments.— We thank Bujiao Wu for insightful discussions. This work is supported by the National Natural Science Foundation of China Grant No. 12175003.

* Electronic address: xiaoyuan@pku.edu.cn

- [1] A. W. Harrow, A. Hassidim, and S. Lloyd, Quantum algorithm for linear systems of equations, *Phys. Rev. Lett.* **103**, 150502 (2009).
- [2] S. Lloyd, M. Mohseni, and P. Rebentrost, Quantum principal component analysis, *Nat. Phys.* **10**, 631 (2014).
- [3] I. Kerendis and A. Prakash, Quantum recommendation systems, [arXiv:1603.08675](https://arxiv.org/abs/1603.08675) (2016).
- [4] A. M. Childs, D. Maslov, Y. Nam, N. J. Ross, and Y. Su, Toward the first quantum simulation with quantum speedup, *Proc. Natl. Acad. Sci.* **115**, 9456 (2018).
- [5] G. H. Low and I. L. Chuang, Hamiltonian simulation by qubitization, *Quantum* **3**, 163 (2019).
- [6] A. Barenco, C. H. Bennett, R. Cleve, D. P. DiVincenzo, N. Margolus, P. Shor, T. Sleator, J. A. Smolin, and H. Weinfurter, Elementary gates for quantum computation, *Phys. Rev. A* **52**, 3457 (1995).
- [7] E. Knill, Approximation by quantum circuits, [arXiv preprint quant-ph/9508006](https://arxiv.org/abs/quant-ph/9508006) (1995).
- [8] J. J. Vartiainen, M. Möttönen, and M. M. Salomaa, Efficient decomposition of quantum gates, *Phys. Rev. Lett.* **92**, 177902 (2004).
- [9] V. V. Shende, I. L. Markov, and S. S. Bullock, Minimal universal two-qubit controlled-not-based circuits, *Phys. Rev. A* **69**, 062321 (2004).
- [10] V. Shende, S. Bullock, and I. Markov, Synthesis of quantum-logic circuits, *IEEE Transactions on Computer-Aided Design of Integrated Circuits and Systems* **25**, 1000 (2006).
- [11] G.-L. Long and Y. Sun, Efficient scheme for initializing a quantum register with an arbitrary superposed state, *Phys. Rev. A* **64**, 014303 (2001).
- [12] L. Grover and T. Rudolph, Creating superpositions that correspond to efficiently integrable probability distributions, [quant-ph/0208112](https://arxiv.org/abs/quant-ph/0208112) (2002).
- [13] M. Möttönen, J. J. Vartiainen, V. Bergholm, and M. M. Salomaa, Transformation of quantum states using uniformly controlled rotations, *Quantum. Inf. Comput.* **5**, 467 (2005).
- [14] V. Bergholm, J. J. Vartiainen, M. Möttönen, and M. M. Salomaa, Quantum circuits with uniformly controlled one-qubit gates, *Phys. Rev. A* **71**, 052330 (2005).
- [15] M. Plesch and Č. Brukner, Quantum-state preparation with uni-

- versal gate decompositions, *Phy. Rev. A* **83**, 032302 (2011).
- [16] R. Iten, R. Colbeck, I. Kukuljan, J. Home, and M. Christandl, Quantum circuits for isometries, *Phys. Rev. A* **93**, 032318 (2016).
- [17] X. Sun, G. Tian, S. Yang, P. Yuan, and S. Zhang, Asymptotically optimal circuit depth for quantum state preparation and general unitary synthesis, [arXiv:2108.06150v2](https://arxiv.org/abs/2108.06150v2) (2021).
- [18] X.-M. Zhang, M.-H. Yung, and X. Yuan, Low-depth quantum state preparation, *Phys. Rev. Research* **3**, 043200 (2021).
- [19] Z. Zhang, Q. Wang, and M. Ying, Parallel quantum algorithm for hamiltonian simulation, [arXiv:2105.11889](https://arxiv.org/abs/2105.11889) (2021).
- [20] G. Rosenthal, Query and depth upper bounds for quantum unitaries via Grover search, [arXiv:2111.07992](https://arxiv.org/abs/2111.07992) (2021).
- [21] E. Tang, A quantum-inspired classical algorithm for recommendation systems, in *Proceedings of the 51st Annual ACM SIGACT Symposium on Theory of Computing* (2019) pp. 217–228.
- [22] N.-H. Chia, A. Gilyén, T. Li, H.-H. Lin, E. Tang, and C. Wang, Sampling-based sublinear low-rank matrix arithmetic framework for dequantizing quantum machine learning, in *Proceedings of the 52nd Annual ACM SIGACT Symposium on Theory of Computing* (2020) pp. 387–400.
- [23] A. Gilyén, Z. Song, and E. Tang, An improved quantum-inspired algorithm for linear regression, [arXiv:2009.07268](https://arxiv.org/abs/2009.07268) (2020).
- [24] N.-H. Chia, T. Li, H.-H. Lin, and C. Wang, Quantum-inspired sublinear algorithm for solving low-rank semidefinite programming, in *45th International Symposium on Mathematical Foundations of Computer Science (MFCS 2020)* (Schloss Dagstuhl-Leibniz-Zentrum für Informatik, 2020).
- [25] E. Malvetti, R. Iten, and R. Colbeck, Quantum circuits for sparse isometries, *Quantum* **5**, 412 (2021).
- [26] T. M. de Veras, L. D. da Silva, and A. J. da Silva, Double sparse quantum state preparation, [arXiv:2108.13527](https://arxiv.org/abs/2108.13527) (2021).
- [27] N. Gleinig and T. Hoefler, An efficient algorithm for sparse quantum state preparation, in *2021 58th ACM/IEEE Design Automation Conference (DAC)* (2021) pp. 433–438.
- [28] T. M. Veras, I. C. De Araujo, K. D. Park, and A. J. Dasilva, Circuit-based quantum random access memory for classical data with continuous amplitudes, *IEEE Transactions on Computers* **70**, 2125 (2021).
- [29] G. Marin-Sanchez, J. Gonzalez-Conde, and M. Sanz, Quantum algorithms for approximate function loading, [arXiv:2111.07933](https://arxiv.org/abs/2111.07933) (2021).
- [30] I. F. Araujo, C. Blank, and A. J. da Silva, Entanglement as a complexity measure for quantum state preparation, [arXiv:2111.03132](https://arxiv.org/abs/2111.03132) (2021).
- [31] See Supplemental Material.
- [32] Y. He, M.-X. Luo, E. Zhang, H.-K. Wang, and X.-F. Wang, Decompositions of n-qubit toffoli gates with linear circuit complexity, *Int. J. Theor. Phys.* **56**, 2350 (2017).
- [33] D. W. Berry, A. M. Childs, R. Cleve, R. Kothari, and R. D. Somma, Simulating hamiltonian dynamics with a truncated taylor series, *Phys. Rev. Lett.* **114**, 090502 (2015).
- [34] S. Chakraborty, A. Gilyén, and S. Jeffery, The power of block-encoded matrix powers: Improved regression techniques via faster Hamiltonian simulation, in *Proceedings of the 46th International Colloquium on Automata, Languages, and Programming*, Leibniz International Proceedings in Informatics, Vol. 132 (2019) pp. 33:1–33:14.
- [35] A. M. Childs, R. Kothari, and R. D. Somma, Quantum algorithm for systems of linear equations with exponentially improved dependence on precision, *SIAM Journal on Computing* **46**, 1920 (2017).
- [36] L. Wossnig, Z. Zhao, and A. Prakash, Quantum linear system algorithm for dense matrices, *Phys. Rev. Lett.* **120**, 050502 (2018).
- [37] J. Biamonte, P. Wittek, N. Pancotti, P. Rebentrost, N. Wiebe, and S. Lloyd, Quantum machine learning, *Nature* **549**, 195 (2017).
- [38] V. Giovannetti, S. Lloyd, and L. Maccone, Quantum random access memory, *Phys. Rev. Lett.* **100**, 160501 (2008).
- [39] V. Giovannetti, S. Lloyd, and L. Maccone, Architectures for a quantum random access memory, *Phys. Rev. A* **78**, 052310 (2008).
- [40] R. Babbush, C. Gidney, D. W. Berry, N. Wiebe, J. McClean, A. Paler, A. Fowler, and H. Neven, Encoding electronic spectra in quantum circuits with linear t complexity, *Phys. Rev. X* **8**, 041015 (2018).
- [41] D. K. Park, F. Petruccione, and J.-K. K. Rhee, Circuit-based quantum random access memory for classical data, *Scientific reports* **9**, 1 (2019).

Supplementary material

I. ARBITRARY QUANTUM STATE PREPARATION

Recall that H is a binary tree of qubits with $(n+1)$ -layer. The l th layer of H is denoted as H_l , and the j th node of H_l is denoted as $H_{l,j}$ ($0 \leq l \leq n$, $0 \leq j \leq 2^l - 1$). We require another n binary trees, each denoted as V_l ($1 \leq l \leq n$). V_l has $(l+1)$ layers, and the m th layer of V_l is denoted as $V_{l,m}$ ($0 \leq m \leq l$). The j th node of $V_{l,m}$ is denoted as $V_{l,m,j}$ ($0 \leq j \leq 2^m - 1$). The leaf $V_{l,l,j}$ is connected to $H_{l,j}$. $V_{l,0}$ corresponds to $V_{l,\text{root}}$ in the main text and $V_{l,l}$ corresponds to $V_{l,\text{leaf}}$ in the main text. The total space complexity is therefore $O(N)$. Before preparation, $H_{0,0}$ is initialized to $|1\rangle$ while all other nodes are initialized to $|0\rangle$.

For target state $\sum_{k=0}^{N-1} \alpha_k |k\rangle$, we define $b_{n,k} \equiv |\alpha_k|$, $b_{l,j} \equiv \sqrt{|b_{l+1,2j}|^2 + |b_{l+1,2j+1}|^2}$ for $0 \leq l \leq n-1$, and $\theta_{l,j} \equiv \arccos(b_{l,2j}/b_{l-1,j})$. It is worthy to note that from the classical description in Eq. (1), compiling the quantum circuit with $O(N)$ space complexity can also be realized with circuit depth $O(n)$, because one can calculate all $\theta_{l,j}$ for same l at circuit depth $O(1)$ in parallel.

The pseudo code of arbitrary state preparation is given in Alg. 1. We have defined $S(\theta, a, b)$ as the two-qubit gate

$$\begin{pmatrix} 1 & & & \\ & \cos \theta & \sin \theta & \\ & \sin \theta & -\cos \theta & \\ & & & 1 \end{pmatrix} \quad (\text{S-1})$$

applied to nodes a and b with basis $\{|00\rangle, |10\rangle, |01\rangle, |11\rangle\}$, and $\text{Ph}(\theta, a)$ as the single qubit phase gate $\begin{pmatrix} 1 & \\ & e^{i\theta} \end{pmatrix}$ applied to node a with basis $\{|0\rangle, |1\rangle\}$. $\text{NOT}(a)$ represents the NOT gate applied to a ; $\text{CNOT}(a; b)$ represents the CNOT gate with a as controlled qubit and b as target qubit; $\text{CCNOT}(a, b; c)$ represents the three-qubit controlled-controlled-NOT gate with a and b as controlled qubits and c as target qubit.

Stage 1. This stage corresponds to line 1-5 in Alg. 1. Take the first and second steps (for loop in line 1 with $l = 1, 2$) as examples, the quantum state for H_0 , H_1 and H_2 follows the transformation

$$|1\rangle_{H_0} |0\rangle_{H_1}^{\otimes 2} |0\rangle_{H_2}^{\otimes 4} \quad (\text{S-2})$$

$$\rightarrow |1\rangle_{H_0} |10\rangle_{H_1} |0\rangle_{H_2}^{\otimes 4} \quad (\text{S-3})$$

$$\rightarrow |1\rangle_{H_0} (b_{1,0}|10\rangle_{H_1} + b_{1,1}|01\rangle_{H_1}) |0\rangle_{H_2}^{\otimes 4} \quad (\text{S-4})$$

$$\rightarrow |1\rangle_{H_0} (b_{1,0}|10\rangle_{H_1} |1000\rangle_{H_2} + b_{1,1}|01\rangle_{H_1} |0010\rangle_{H_2}) \quad (\text{S-5})$$

$$\rightarrow |1\rangle_{H_0} (b_{1,0}|10\rangle_{H_1} \left(\frac{b_{2,0}}{b_{1,0}} |1000\rangle_{H_2} + \frac{b_{2,1}}{b_{1,0}} |0100\rangle_{H_2} \right) + b_{1,1}|01\rangle_{H_1} \left(\frac{b_{2,2}}{b_{1,1}} |0010\rangle_{H_2} + \frac{b_{2,3}}{b_{1,1}} |0001\rangle_{H_2} \right)) \quad (\text{S-6})$$

$$= \sum_{k=0}^{2^2-1} b_{2,k} |1\rangle_{H_0} \bigotimes_{l=1}^2 |(k, l)\rangle'_{H_l}. \quad (\text{S-7})$$

Similarly, after the n th step, the quantum state of H becomes

$$\sum_{k=0}^{2^n-1} b_{n,k} |1\rangle_{H_0} \bigotimes_{l=1}^n |(k, l)\rangle'_{H_l}. \quad (\text{S-8})$$

After implementing line 5 of Alg. 1, we obtain

$$\sum_{k=0}^{2^n-1} a_k |1\rangle_{H_0} \bigotimes_{l=1}^n |(k, l)\rangle'_{H_l}, \quad (\text{S-9})$$

which is Eq. (2) in the main text. Each step of this stage have circuit depth $O(1)$, so the total circuit depth is $O(n)$.

Stage 2. This stage corresponds to lines 6-8 of Alg. 1 with PCNOT the parallel CNOT gates described in Sec. IA (Alg. 2). The goal of this stage is to perform the transformation $|(k, l)\rangle'_{H_l} |0\rangle_{V_{l,0}} \rightarrow |(k, l)\rangle'_{H_l} |k_{n-l+1}\rangle_{V_{l,0}}$.

We suppose the excitation at layer H_l is $H_{l,j_{\text{ex}}(l)}$. For Eq. (S-9), it can be noticed that if $j_{\text{ex}}(l)$ is an even, $|k_{n-l+1}\rangle = |0\rangle$; and if $j_{\text{ex}}(l)$ is an odd, $|k_{n-l+1}\rangle = |1\rangle$. As an example, for $|k\rangle = |1010\rangle$, we have $|(1010, 1)\rangle' = |1\rangle' = |01\rangle$, $|(1010, 2)\rangle' = |10\rangle' = |0010\rangle$, $|(1010, 3)\rangle' = |101\rangle' = |0000100\rangle$, $|(1010, 4)\rangle' = |1010\rangle' = |000000000100000\rangle$. The excitation nodes at each layer corresponds to $j_{\text{ex}}(1) = 1$ (odd), $j_{\text{ex}}(2) = 2$ (even), $j_{\text{ex}}(3) = 5$ (odd), $j_{\text{ex}}(4) = 10$ (even). Accordingly, we have $|k_{4-1+1}\rangle = |1\rangle$, $|k_{4-2+1}\rangle = |0\rangle$, $|k_{4-3+1}\rangle = |1\rangle$, $|k_{4-4+1}\rangle = |0\rangle$.

Based on the observation above, one just need to flip $V_{l,0}$ when the excitation at H_l corresponds to an odd $j_{\text{ex}}(l)$, which is the consequence of this stage. We therefore obtain

$$\sum_{k=0}^{2^n-1} a_k |1\rangle_{H_0} \bigotimes_{l=1}^n |(k, l)\rangle'_{H_l} |k_{n-l+1}\rangle_{V_{l,0}}. \quad (\text{S-10})$$

Lines 6, 8 of Alg. 1 has circuit depth $O(1)$, and line 7 has circuit depth $O(n)$. So this stage has circuit depth $O(n)$.

Stage 3. This stage corresponds to line 9 of Alg. 1 (see also Alg. 3 in Sec. IA). The fanout operation ‘‘copy’’ the state at the root of V_l to the leaves of V_l . According to Eq. (S-19), the quantum state of H , $V_{l,0}$ and $V_{l,l}$ for all $0 \leq j \leq 2^l - 1$ becomes

$$\sum_{k=0}^{2^n-1} a_k |1\rangle_{H_0} \bigotimes_{l=1}^n |(k, l)\rangle'_{H_l} |k_{n-l+1}\rangle_{V_{l,0}} |k_{n-l+1}\rangle_{V_{l,l}}^{\otimes 2^l}. \quad (\text{S-11})$$

Because the fanout operation for each l can be implemented in parallel, the circuit depth of this stage is $O(n)$.

Stage 4. This stage corresponds to line 10-16 of Alg. 1, and our goal is to uncompute H . In each basis of Eq. (S-11), we have

$$H_{l,2j} \text{ is excited} \iff V_{l,l,2j} \text{ is not excited, and } H_{l-1,j} \text{ is excited} \quad (\text{S-12})$$

$$H_{l,2j+1} \text{ is excited} \iff \text{both } V_{l,l,2j+1} \text{ and } H_{l-1,j} \text{ are excited} \quad (\text{S-13})$$

So line 11 and 12 uncomputes $H_{l,2j}$ and $H_{l,2j+1}$ respectively. With total circuit depth $O(n)$, the quantum state after this stage becomes

$$\sum_{k=0}^{2^n-1} a_k |1\rangle_{H_0} \bigotimes_{l=1}^n |0\rangle_{H_l}^{\otimes 2^l} |k_{n-l+1}\rangle_{V_{l,0}} |k_{n-l+1}\rangle_{V_{l,l}}^{\otimes 2^l}. \quad (\text{S-14})$$

Stage 5. This stage corresponds to line 17 of Alg. 1, after which we obtain

$$\sum_{k=0}^{2^n-1} a_k |1\rangle_{H_0} \bigotimes_{l=1}^n |0\rangle_{H_l}^{\otimes 2^l} |k_{n-l+1}\rangle_{V_{l,0}} |0\rangle_{V_{l,l}}^{\otimes 2^l}. \quad (\text{S-15})$$

By tracing out all nodes except for $V_{l,0}$ for $l \in \{1, \dots, n\}$, we obtain

$$\sum_{k=0}^{2^n-1} a_k \bigotimes_{l=1}^n |k_{n-l+1}\rangle_{V_{l,0}}. \quad (\text{S-16})$$

Because $|k\rangle \equiv |k_n k_{n-1}, \dots, k_1\rangle$, Eq. (S-16) is equivalent to the target state Eq. (1) with $V_{l,0}$ being the $(n-l+1)$ th digit.

To sum up, the target state is prepared with totally $\Theta(n)$ circuit depth, saturating the lower bound. Note that for reaching the circuit depth $\Theta(n)$, at least $\Omega(N/n)$ ancillary qubits are required. So the space complexity $O(N)$ of our method is near-optimal.

A. Parallel CNOT gate and fanout operation based on binary tree

Given an $(L+1)$ -layer binary tree T (each node represents a qubit), we denote its l th ($0 \leq l \leq L$) layer as T_l , and the j th node ($0 \leq j \leq 2^l - 1$) at the l th layer as $T_{l,j}$. The parallel CNOT (PCNOT) gate is described in Alg. 2. Note that the operations at each line can be realized at circuit depth $O(1)$. To see how it works, we consider a subspace with all $T_{l,j}$ for $1 \leq l \leq L-1$ at $|0\rangle$, and there is either zero or single excitation at T_L . The available basis for T_L is $\mathcal{L} = \{|\text{vac}\rangle', |0\rangle', |1\rangle' \dots |2^L - 1\rangle'\}$, where

$|\text{vac}\rangle' \equiv |0\rangle^{\otimes 2^L}$ and $|j\rangle' \equiv |0\rangle^{\otimes j}|1\rangle|0\rangle^{\otimes 2^L-j-1}$, and the basis for $T_{0,0}$ is $\{|0\rangle, |1\rangle\}$. We have

$$\text{PCNOT}(T)|z\rangle_{T_0}|j\rangle'_{T_L} = |\bar{z}\rangle_{T_0}|j\rangle'_{T_L} \quad \text{for } |j\rangle'_{T_L} \neq |\text{vac}\rangle_{T_L}, \quad (\text{S-17})$$

$$\text{PCNOT}(T)|z\rangle_{T_0}|j\rangle'_{T_L} = |z\rangle_{T_0}|j\rangle'_{T_L} \quad \text{for } |j\rangle'_{T_L} = |\text{vac}\rangle_{T_L}. \quad (\text{S-18})$$

In other words, we flip the root if there is an excitation at the leaf.

The fanout operation for T is described in Alg. 3. In the same subspace above for PCNOT, we have

$$\text{Fanout}(T)|z\rangle_{T_0}|\text{vac}\rangle_{T_L} = |z\rangle_{T_0}|z\rangle_{T_L}^{\otimes 2^L}, \quad (\text{S-19})$$

$$\text{Fanout}(T)|z\rangle_{T_0}|z\rangle_{T_L}^{\otimes 2^L} = |z\rangle_{T_0}|\text{vac}\rangle_{T_L}. \quad (\text{S-20})$$

Each step in Alg. 2 and Alg. 3 can be realized with circuit depth $O(1)$, so both operations have total circuit depth $O(L)$.

Algorithm 1 : Arbitrary quantum state preparation

Input: rotation angles $\theta_{l,j}$ for $1 \leq l \leq n$ and $0 \leq j \leq 2^l - 1$; phase angles $\arg(a_k)$ for $0 \leq k \leq 2^n - 1$

Require: Binary trees H and V_l for all $1 \leq l \leq n$ with all nodes initialized as $|0\rangle$ except for $H_{0,0}$ as $|1\rangle$

Output: quantum state described in Eq. (1) with $V_{l,0}$ being the $(n-l+1)$ th digit

- 1: **for** $l = 1$ to n :
 - 2: CNOT ($H_{l-1,j}, H_{l,2j}$) for all $0 \leq j \leq 2^{l-1} - 1$
 - 3: $S(\theta_{l,j}, H_{l,2j}, H_{l,2j+1})$ for all $0 \leq j \leq 2^{l-1} - 1$
 - 4: **end**
 - 5: Ph($\arg(a_j), H_{n,j}$) for all $0 \leq j \leq 2^n - 1$
 - 6: CNOT($H_{l,j}; V_{l,l,j}$) for all $1 \leq l \leq n$ and $j \in \{1, 3, 5 \dots 2^l - 1\}$
 - 7: PCNOT(V_l) for all $1 \leq l \leq n$
 - 8: CNOT($H_{l,j}; V_{l,l,j}$) for all $1 \leq l \leq n$ and $j \in \{1, 3, 5 \dots 2^l - 1\}$
 - 9: Fanout(V_l) for all $1 \leq l \leq n$
 - 10: **for** $l' = 1$ to n :
 - 11: Let $l = n - l' + 1$
 - 12: NOT($V_{l,l,2j}$) for all $j \in \{0, 1, 2 \dots 2^{l-1} - 1\}$
 - 13: CCNOT($V_{l,l,2j}, H_{l-1,j}; H_{l,2j}$) for all $j \in \{0, 1, 2 \dots 2^{l-1} - 1\}$
 - 14: NOT($V_{l,l,2j}$) for all $j \in \{0, 1, 2 \dots 2^{l-1} - 1\}$
 - 15: CCNOT($V_{l,l,2j+1}, H_{l-1,j}; H_{l,2j+1}$) for all $j \in \{0, 1, 2 \dots 2^{l-1} - 1\}$
 - 16: **end**
 - 17: Fanout(V_l) for all $1 \leq l \leq n$
-

Algorithm 2 : PCNOT(T)

- 1: **for** $l' = 0$ to $L - 1$:
 - 2: Let $l = L - l'$
 - 3: CNOT ($T_{l,j}; T_{l-1,j/2}$) for all $j \in \{0, 2, 4 \dots 2^l - 2\}$
 - 4: CNOT ($T_{l,j}; T_{l-1,(j-1)/2}$) for all $j \in \{1, 3, 5 \dots 2^l - 1\}$
 - 5: **end**
 - 6: **for** $l' = 0$ to $L - 2$:
 - 7: Let $l = L - l'$
 - 8: CNOT ($T_{l,j}; T_{l-1,j/2}$) for all $j \in \{0, 2, 4 \dots 2^l - 2\}$
 - 9: CNOT ($T_{l,j}; T_{l-1,(j-1)/2}$) for all $j \in \{1, 3, 5 \dots 2^l - 1\}$
 - 10: **end**
-

Algorithm 3 : Fanout(T)

```

1: for  $l = 0$  to  $L - 1$ :
2:   CNOT ( $T_{l,j}; T_{l+1,2j}$ ) for all  $0 \leq j \leq 2^l - 1$ 
3:   CNOT ( $T_{l,j}; T_{l+1,2j+1}$ ) for all  $0 \leq j \leq 2^l - 1$ 
4: end
5: for  $l = 0$  to  $L - 2$ :
6:   CNOT ( $T_{l,j}; T_{l+1,2j}$ ) for all  $0 \leq j \leq 2^l - 1$ 
7:   CNOT ( $T_{l,j}; T_{l+1,2j+1}$ ) for all  $0 \leq j \leq 2^l - 1$ 
8: end

```

II. CIRCUIT DEPTH LOWER BOUND FOR SPARSE STATE PREPARATION

Lemma 3. *With only single- and two-qubit gates and arbitrary amount of ancillary qubits, the minimum circuit depth of preparing arbitrary d -sparse ($d \geq 2$) quantum states is $\Omega(\log(nd))$.*

Proof. Firstly, we consider the preparation of the GHZ state $1/\sqrt{2}(|0\rangle^{\otimes n} + |1\rangle^{\otimes n})$, which can be considered as a d -sparse state with any $d \geq 2$. For initial state $|0\rangle^{\otimes n}$, there is no correlation between each qubit, while in the target GHZ state, each qubit is correlated to all other qubits. To establish the correlations between one qubit to all other $n - 1$ qubits with single- and two-qubit gates, $\Omega(\log n)$ circuit depth is necessary.

Secondly, when preparing an n -qubit state with a L -depth quantum circuit using only single- and two-qubit gates, there are at most $O(n \cdot 2^L)$ effective parameters (Ref [17], Lemma 28). On the other hand, specifying a d -sparse ($2 \leq d \leq 2^n$) quantum state requires no less than $\Omega(d)$ parameters. Therefore, to prepare arbitrary d -sparse quantum states, the circuit depth is lower bounded by $\Omega(\log(d/n)) = \Omega(\log d - \log n)$.

Combining results above, the circuit lower bound is $\Omega(\log(nd))$. \square

The derivation above also indicates that to reach the circuit depth $\Theta(\log(nd))$, at least $\Omega(d - n)$ ancillary qubits are required. If we further consider the resource for storing the values and indexes of all nonzero entries, the total space complexity is lower bounded by $\Omega(nd)$.

III. PRODUCT UNITARY MEMORY (PUM) AND SPARSE BOOLEAN MEMORY (SBM)

In this section, we provide details about the data structure introduced in Lemma 1 (PUM) and Lemma 2 (SBM). We begin with single-word cases in Sec. III A (PUM) and Sec. III B (SBM). Then, in Sec. III C, we discuss how to generalize PUM and SBM to multi-word cases.

A. Single-word PUM

In this subsection, our goal is to perform the transformation

$$\text{select}(\hat{U}) \sum_{k=0}^{d-1} \sum_{z=0,1} \psi_{k,z} |k\rangle |z\rangle = \sum_{k=0}^{d-1} \sum_{z=0,1} \psi_{k,z} |k\rangle \hat{U}(k) |z\rangle, \quad (\text{S-21})$$

where $|k\rangle$ is the \tilde{n} -qubit basis ($d = 2^{\tilde{n}}$) of the index register and $|z\rangle$ is the basis of the single-qubit word register. We will introduce the main idea of our protocol in Sec. III A 1 and then provide the formal description in Sec. III A 2.

1. Main idea

The element of the architecture is the *router* containing four qubits. If we denote the incident qubit, routing qubit, left output qubit and right output qubit as q_{incident} , q_{route} , q_{left} and q_{right} respectively, the *routing* operation is defined as

$$\text{NOT}(q_{\text{route}}) \text{CSWAP}(q_{\text{route}}; q_{\text{incident}}, q_{\text{left}}) \text{NOT}(q_{\text{route}}) \text{CSWAP}(q_{\text{route}}; q_{\text{incident}}, q_{\text{right}}). \quad (\text{S-22})$$

By applying the routing operation, the state of q_{incident} is transferred to q_{left} (q_{right}) of the same router if the routing qubit is at state $|0\rangle$ ($|1\rangle$).

The single-word PUM has $(2d - 1)$ routers arranged as a \tilde{n} -layer binary tree, a pointer qubit and totally d memory cells. Each left (right) output qubit serves as the incident qubit of its left (right) child. Each left and right output qubit of the node at the leaf layer connects to a memory cell. Each memory cell contains a control-holder qubit and a word-holder qubit initialized as $|0\rangle$. The k th memory cell stores classically the single qubit unitary $U(k)$.

Our method has three stages. In the route-in stage, the state of index register, word register and pointer qubit (initialized as $|1\rangle$) are sent into the binary tree sequentially. The *routing* operation [Eq. (S-22)] transfer the state of the incident qubit a node to the incident qubit of its left (right) child, conditioned on the routing qubit is at state $|0\rangle$ ($|1\rangle$). The state of the l th index qubit is finally transferred to one of the routing qubits at the l th layer. The states of the word register and the pointer qubit travels to the word-holder and pointer-holder qubits of the k th memory cell, conditioned on the intup index register at state $|k\rangle$.

In the query stage, at the k th memory cell, we implement controlled- $\hat{U}(k)$ with pointer-holder as controlled qubit and the word-holder as target qubit. This gives either the transformation $|z\rangle|1\rangle \rightarrow \hat{U}(k)|z\rangle|1\rangle$ or $|00\rangle \rightarrow |00\rangle$.

In the route-out stage, we perform the inverse of the route-in stage. The index register, word register and the pointer qubit are transferred to the state $\sum_{k=0}^{d-1} \psi_{k,z}|k\rangle U(k)|z\rangle|1\rangle$, while all other qubits are uncomputed. By tracing out the pointer qubit, we obtain the target state.

2. Formal description

We denote the j th router at the l th layer as $R_{l,j}$, the pointer holder and word holder at the k th memory cell as phd_k and whd_k . We defined several operations required by our protocol as follow:

- **Input(m):** swap gate between the m th qubit at the index register and the incident qubit of $R_{0,0}$
- **Input(pointer):** swap gate between pointer qubit, and the incident qubit of $R_{0,0}$
- **Input(word):** swap gate between the qubit at word register and the incident qubit of $R_{0,0}$
- **Route(l):** routing operation defined in Eq (S-22) for all routers $R_{l,j}$ with $j \in \{0, 2^l - 1\}$
- **Set(l):** swap gate between the incident qubit and routing qubit of $R_{l,j}$ for all $j \in \{0, 1, \dots, 2^l - 1\}$
- **Output(pointer):** swap gate between $R_{\tilde{n},k}$ and the pointer holder phd_k for all $k \in \{0, 1 \dots d - 1\}$
- **Output(word):** swap gate between $R_{\tilde{n},k}$ and the word-holder qubit whd_k for all $k \in \{0, 1 \dots d - 1\}$
- **CU($\text{phd}_k; \text{whd}_k$):** Controlled- $U(k)$ with phd_k as controlled qubit and whd_k as target qubit for all $k \in \{0, 1 \dots d - 1\}$

Note that each operation above can be implemented with circuit depth $O(1)$. The pseudo code for the full process is given in Alg. 4, and the route-in stage is given in Alg. 5, where we have assumed that $\tilde{n}/6$ is an integer.

Algorithm 4 : select(\hat{U}) for single-word case

- 1: Route-in
 - 2: CU($\text{phd}_k; \text{whd}_k$) for all $k \in \{0, 1 \dots d - 1\}$
 - 3: inverse of Route-in
-

Algorithm 5 : Route-in

```

1: for  $L = 1$  to  $\tilde{n}/3$ 
2:   Input( $3L - 2$ ); Route( $2l$ ) for all  $1 \leq l \leq (L - 1)$ 
3:   Route( $2l - 1$ ) for all  $1 \leq l \leq (L - 1)$ ; Set( $2L - 1$ )
4:   Input( $3L - 1$ ); Route( $2l$ ) for all  $1 \leq l \leq (L - 1)$ 
5:   Route( $2l - 1$ ) for all  $1 \leq l \leq L$ 
6:   Input( $3L$ ); Route( $2l$ ) for all  $1 \leq l \leq (L - 1)$ ; Set( $2L$ )
7:   Route( $2l - 1$ ) for all  $1 \leq l \leq L$ 
8: end
9: Input(pointer); Route( $2l$ ) for all  $1 \leq l \leq \tilde{n}/3$ 
10: Route( $2l - 1$ ) for all  $1 \leq l \leq \tilde{n}/3$ ; Set( $2\tilde{n}/3 + 1$ )
11: Input(word); Route( $2l$ ) for all  $1 \leq l \leq \tilde{n}/3$ 
12: for  $L = \tilde{n}/3 + 1$  to  $\tilde{n}/2 - 1$ 
13:   Route( $2l - 1$ ) for all  $(3L - \tilde{n} - 2) \leq l \leq L$ 
14:   Route( $2l$ ) for all  $(3L - \tilde{n} - 2) \leq l \leq (L - 1)$ ; Set( $2L$ )
15:   Route( $2l - 1$ ) for all  $(3L - \tilde{n} - 1) \leq l \leq L$ 
16:   Route( $2l$ ) for all  $(3L - \tilde{n} - 1) \leq l \leq L$ 
17:   Route( $2l - 1$ ) for all  $(3L - \tilde{n}) \leq l \leq L$ ; Set( $2L + 1$ );
18:   Route( $2l$ ) for all  $(3L - \tilde{n}) \leq l \leq L$ ;
19: end
20: Route( $2l - 1$ ) for all  $(\tilde{n}/2 - 2) \leq l \leq \tilde{n}/2$ 
21: Route( $2l$ ) for all  $(\tilde{n}/2 - 3) \leq l \leq (\tilde{n}/2 - 1)$ ; Set( $\tilde{n}$ )
22: Route( $2l - 1$ ) for all  $(\tilde{n}/2 - 1) \leq l \leq \tilde{n}/2$ 
23: Route( $\tilde{n} - 2$ ); Output(pointer)
24: Route( $\tilde{n} - 1$ )
25: Output(word)

```

B. Single-word sparse Boolean memory (SBM)

In this subsection, our goal is to perform the transformation

$$\sum_{k=0}^{2^n-1} \sum_{z=0,1} \psi_k |k\rangle |z\rangle \longrightarrow \sum_{k=0}^{2^n-1} \sum_{z=0,1} \psi_k |k\rangle |z \oplus f(k)\rangle, \quad (\text{S-23})$$

where $|k\rangle$ is the state of the n -qubit index register, and $|z\rangle$ is the state of single-qubit word register. Without loss of generality, we assume that both $L_s \equiv \log_2 s$ (recall that $f(k)$ is s -sparse) and $L_n \equiv \log_2 n$ are integers. If L_n is not, we add extra qubits with state $|0\rangle$ to the index register until the assumption is satisfied.

For each $l \in \{1, 2, \dots, n\}$, we introduce a L_s -layer binary tree (index tree) denoted as T_l^{idx} . We denote the m th layer of T_l^{idx} as $T_{l,m}^{\text{idx}}$, and the w th node of $T_{l,m}^{\text{idx}}$ as $T_{l,m,w}^{\text{idx}}$. The l th qubit of index register serves as the root $T_{l,0,0}^{\text{idx}}$. Let $\mathcal{S}_f = \{r_0, r_1, \dots, r_{s-1}\}$ be a set containing all indexes satisfying $f(r_w) = 1$. Our structure has totally s memory cells. The w th cell stores r_w and each cell contains a L_n -layer binary tree (memory tree) T_w^{cell} . Similarly, the m th layer of T_w^{cell} is $T_{w,m}^{\text{cell}}$, and the j th node of T_w^{cell} is $T_{w,m,j}^{\text{cell}}$. The memory trees and index trees share their leaves. More specifically, we have $T_{w,L_n,l}^{\text{cell}} = T_{l,L_s,w}^{\text{idx}}$. The word holders introduced in the main text are the roots of memory trees $T_{w,0,0}^{\text{cell}}$. We then introduce another L_s -layer binary tree (word tree) $T^{\text{wrđ}}$. Its w th node at the m th layer is denoted as $T_{m,w}^{\text{wrđ}}$. It connects all word holders to the word register, i.e. $T_{0,0}^{\text{wrđ}}$ is the word register and $T_{L_s,w}^{\text{wrđ}} = T_{w,0,0}^{\text{cell}}$.

The algorithm is shown in Alg. 6. The first step is line 1 of Alg. 6, which fanouts the state of index register $|k\rangle$ to the index holders at each memory cell. The quantum state becomes

$$\sum_{k=0}^{2^n-1} \sum_{z=0,1} \psi_{k,z} |k\rangle |z\rangle (|k\rangle |0\rangle)^{\otimes s}. \quad (\text{S-24})$$

The second step is line 2 of Alg. 6. We apply the n -Toffoli gates defined in Alg. 7. The transformation $|k\rangle |0\rangle \rightarrow |k\rangle |k = r_w\rangle$ is

performed in each memory cell, so the state becomes.

$$\sum_{k=0}^{2^n-1} \sum_{z=0,1} \psi_{k,z} |k\rangle |z\rangle \bigotimes_{w=0}^{s-1} |k\rangle |k = r_w\rangle. \quad (\text{S-25})$$

The third step is line 3 of Alg. 6. There are at most one excitation at the leaf layer of T^{word} , so the parallel CNOT gate (defined in Alg. 2) performs the transformation $|z\rangle \rightarrow |z \oplus \prod_{w=0}^{s-1} (k = r_w)\rangle = |z \oplus f(k)\rangle$, and the quantum state becomes

$$\sum_{k=0}^{2^n-1} \sum_{z=0,1} \psi_{k,z} |k\rangle |z \oplus f(k)\rangle \bigotimes_{w=0}^{s-1} |k\rangle |k = r_w\rangle. \quad (\text{S-26})$$

The fourth step is line 4,5 of Alg. 6, aiming at uncomputing T_w^{cell} . After this step, the final state becomes

$$\sum_{k=0}^{2^n-1} \sum_{z=0,1} \psi_{k,z} |k\rangle |z \oplus f(k)\rangle (|0\rangle^{\otimes n} |0\rangle)^{\otimes s}. \quad (\text{S-27})$$

By tracing out the index holders and word holders, we obtain the target state.

Step 1 and 3 have circuit depth $O(\log s)$, step 2 have circuit depth $O(\log n)$, and step 4 have circuit depth $O(\log s + \log n)$. Therefore, the total circuit depth of single-word SBM is $O(\log(sn))$.

Algorithm 6 : $\text{select}(f)$ for single-word case

- 1: Fanout(T_l^{idx}) for all $l \in \{1, 2, \dots, n\}$
 - 2: Toffoli(r_w, T_w^{cell}) for all $w \in \{0, 1, \dots, s-1\}$
 - 3: PCNOT(T^{orc})
 - 4: Toffoli(r_w, T_w^{cell}) for all $k \in \{0, 1, \dots, s-1\}$
 - 5: Fanout(T_l^{idx}) for all $l \in \{1, 2, \dots, n\}$
-

Algorithm 7 : Toffoli(r_w, T_w^{cell})

- 1: NOT($T_{w,L_n,j}^{\text{cell}}$) for all $r_{w,j} = 0$ # $r_{w,j}$ represents the $(j+1)$ th digit of r_w
 - 2: CCNOT($T_{w,L_n,2j}^{\text{cell}}, T_{w,L_n,2j+1}^{\text{cell}}; T_{w,L_n-1,j}^{\text{cell}}$) for all $j \in \{0, 1, \dots, n/2-1\}$
 - 3: **for** $\tilde{m} = 1$ to $L_n - 1$:
 - 4: $m = L_n - \tilde{m}$
 - 5: CCNOT($T_{w,m,2j}^{\text{cell}}, T_{w,m,2j+1}^{\text{cell}}; T_{w,m-1,j}^{\text{cell}}$) for all $j \in \{0, 1, \dots, 2^{m-1} - 1\}$
 - 6: **end**
 - 7: **for** $\tilde{m} = 1$ to $L_n - 2$:
 - 8: $m = L_n - \tilde{m}$
 - 9: CCNOT($T_{w,m,2j}^{\text{cell}}, T_{w,m,2j+1}^{\text{cell}}; T_{w,m-1,j}^{\text{cell}}$) for all $j \in \{0, 1, \dots, 2^{m-1} - 1\}$
 - 10: **end**
 - 11: CCNOT($T_{w,L_n,2j}^{\text{cell}}, T_{w,L_n,2j+1}^{\text{cell}}; T_{w,L_n-1,j}^{\text{cell}}$) for all $j \in \{0, 1, \dots, n/2-1\}$
 - 12: NOT($T_{w,L_n,j}^{\text{cell}}$) for all $r_{w,j} = 0$
-

C. Multi-word cases for PUM and SBM

In below, we discuss the generalization of PUM and SBM to multi-word cases. The basic idea is to implement fanout (Alg. 3) to obtain multiple ‘‘copies’’ of index register, and then query the oracles for different words in parallel, and then implement fanout again for uncomputation. We take PUM for Lemma 1 as an example, and same idea can be straightforwardly applied to SBM for Lemma 2.

For PUM with $n \geq 1$, we introduce another n registers, and denote the l th register as I_l . Each I_l contains \tilde{n} ancillary qubits with initial state $|0\rangle^{\otimes \tilde{n}}$. The basis of word register is $|z\rangle \equiv |z_n\rangle \cdots |z_2\rangle |z_1\rangle$. We can represent the input state of the PUM as

$$\sum_{k=0}^{d-1} \sum_{z=0}^{2^n-1} \psi_{k,z} |k\rangle \bigotimes_{l=1}^L |0\rangle_{I_l}^{\otimes \tilde{n}} |z_l\rangle. \quad (\text{S-28})$$

The entire query process is illustrate in Fig S1. In the first step, we fanout the state of index register to each I_l , and obtain

$$\sum_{k=0}^{d-1} \sum_{z=0}^{2^n-1} \psi_{k,z} |k\rangle \bigotimes_{l=1}^n |k\rangle_{I_l} |z_l\rangle. \quad (\text{S-29})$$

In the second step, we query single-word PUMs $\text{select}(\hat{U}_l)$ for all $1 \leq l \leq n$ in parallel with $|k\rangle_{I_l} |z_l\rangle$ as the input state. The output state is

$$\sum_{k=0}^{d-1} \sum_{z=0}^{2^n-1} \psi_{k,z} |k\rangle \bigotimes_{l=1}^n \text{select}(\hat{U}_l) |k\rangle_{I_l} |z_l\rangle \quad (\text{S-30})$$

$$= \sum_{k=0}^{d-1} \sum_{z=0}^{2^n-1} \psi_{k,z} |k\rangle \bigotimes_{l=1}^n |k\rangle_{I_l} \hat{U}_l(k) |z_l\rangle. \quad (\text{S-31})$$

Finally, we repeat the fanout operation in the first step to uncompute I_l . The state then becomes

$$\sum_{k=0}^{d-1} \sum_{z=0}^{2^n-1} \psi_{k,z} |k\rangle \bigotimes_{l=1}^n |0\rangle_{I_l}^{\otimes \tilde{n}} \hat{U}_l(k) |z_l\rangle. \quad (\text{S-32})$$

By tracing out registers I_l and noticing that $U(k) = \bigotimes_{l=1}^n U_l(k)$, we obtain

$$\sum_{k=0}^{d-1} \sum_{z=0}^{2^n-1} \psi_{k,z} |k\rangle \bigotimes_{l=1}^n \hat{U}_l(k) |z_l\rangle \quad (\text{S-33})$$

$$= \sum_{k=0}^{d-1} \sum_{z=0}^{2^n-1} \psi_{k,z} |k\rangle \hat{U}(k) |z\rangle, \quad (\text{S-34})$$

which is the expected output. The fanout operation has $O(\log n)$ circuit depth, and the parallel query of each $\text{select}(\hat{U}_l)$ has circuit depth $O(\log d)$. So the total circuit depth is $O(\log(nd))$. Because each $\text{select}(\hat{U}_l)$ requires $O(d)$ ancillary qubits and they are queried in parallel, $\text{select}(\hat{U}_l)$ requires totally $O(nd)$ ancillary qubits. So Lemma. 1 holds true.

We can apply the similar method to generalize SBM for $\tilde{n} > 1$. In that case, the total circuit depth is $O(\log(ns\tilde{n}))$ and $O(ns\tilde{n})$ ancillary qubits are required. So Lemma. 2 holds true.

IV. HAMILTONIAN SIMULATION BASED ON QUBITIZATION

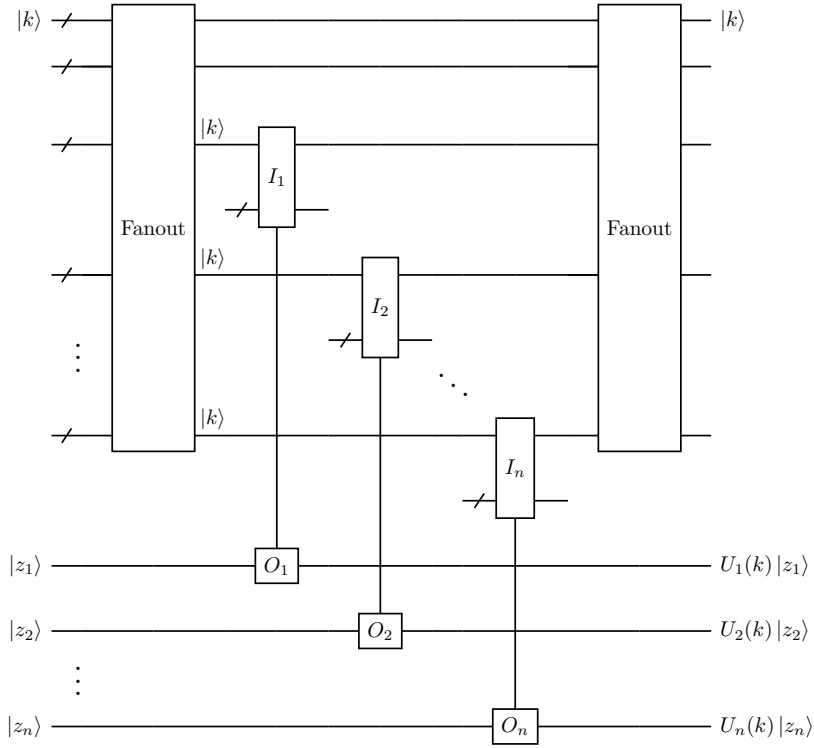
According to Ref. [5], Hamiltonian simulation can be realized with block-encoding.

Lemma 4 (Theorem 1 in Ref. [5]). *Let $(\langle G | \otimes \hat{\mathbb{I}}_L) \hat{U} (|G\rangle \otimes \hat{\mathbb{I}}_L) = \hat{H}/\alpha \in \mathbb{C}^{2^n \otimes 2^n}$ be Hermitian for some unitary $\hat{U} \in \mathbb{C}^{(P^{2^n}) \times (P^{2^n})}$ and some state preparation unitary $\hat{G}|0\rangle = |G\rangle \in \mathbb{C}^P$ and $\alpha > 0$. Then $e^{-i\hat{H}t}$ can be simulated for time t , error ε in spectral norm, and failure probability $O(\varepsilon)$, using at most $\Theta(\alpha t + \log(1/\varepsilon))$ queries to controlled- \hat{G} , controlled- \hat{U} , and their inverses, $O((\alpha t + \log(1/\varepsilon)) \log(P))$ additional two-qubit quantum gates, and $O(n + \log(P))$ extra qubits.*

The total circuit depth and space complexity are subject to the cost of querying \hat{G} and \hat{U} . Theorem. 3 in the main text follows directly from Lemma. 4.

Proof of Theorem. 3. Let \hat{G} be a unitary satisfying $\hat{G}|0\rangle^{\otimes \lceil \log_2 P \rceil} = \sum_{p=0}^{P-1} \alpha_p |p\rangle$. It can be verified that

$$\left(\langle 0 |^{\otimes \lceil \log_2 P \rceil} \hat{G}^\dagger \otimes \hat{\mathbb{I}}_n \right) \text{select}(\hat{V}) \left(\hat{G} |0\rangle^{\otimes \lceil \log_2 P \rceil} \otimes \hat{\mathbb{I}}_n \right) = \hat{H}/\alpha. \quad (\text{S-35})$$



Supplementary Figure S1: The query of multi-word PUM is realized by querying many single-word PUM in parallel. I_l represents the index register part of the single-word oracle $\text{select}(\hat{U}_l)$, and O_l represents the word register part of the single-word oracle $\text{select}(\hat{U}_l)$.

According to Theorem 1, implementing \hat{G} requires circuit depth $O(\log P)$ and $O(P)$ ancillary qubits. According to Lemma 1, implementing $\text{select}(\hat{V})$ requires circuit depth $O(\log(nP))$ and $O(nP)$ ancillary qubits. Combining these results with Lemma 4, Theorem 3 holds true. \square

V. PARALLEL HAMILTONIAN SIMULATION BASED ON QUANTUM WALK

In Ref. [19], the authors developed a parallel algorithm to improve the circuit depth to doubly logarithmic dependence on the precision ε . Their protocol is based on the access of two oracles

$$O_H^b |i\rangle |j\rangle |z\rangle = |i\rangle |j\rangle |z \oplus H_{i,j}\rangle \quad (\text{S-36})$$

$$O_L |i\rangle |k\rangle = |i\rangle |L(i, k)\rangle \quad (\text{S-37})$$

where i and j are the row and column indexes of \hat{H} , b is the precision of H , $|z\rangle$ is a b -bit basis, \oplus is the bit-wise XOR, and $L(i, k)$ represents the column index of the k th non-zero element in row i . As an example, we focus on Hamiltonians in the form of Eq. (6) in the main text with $\hat{V}_l(p)$ restricted to be Pauli operators (although a more general model has been discussed in [19]). In this case, O_H^b and O_L can be realized with circuit depth $O(nb)$ and $O(n)$ respectively.

The goal is to simulate the evolution $e^{-i\hat{H}t}$ to precision ε . According to Ref. [19], the simulation can be implemented with $O(\tau \log(\gamma))$ depth of query to O_H^b and O_L , $O(1)$ depth query to the quantum state preparation unitary for $O(\gamma)$ dimensional states, and $O(\tau \log^2 \gamma \log^2 n)$ extra depth of single- and two-qubit gates. We have assumed $P = O(\text{poly}(n))$, and defined $\tau \equiv Pt$ and $\gamma \equiv \log(\tau/\varepsilon)$. Ref. [19] uses a quantum state preparation method with circuit depth $O(\log^3 \gamma)$, achieving the total circuit depth

$$O\left(\tau \left(\log^2 \gamma \log^2 n + \log^3 \gamma\right)\right). \quad (\text{S-38})$$

On the other hand, with our optimal protocol, the circuit depth for state preparation can be improved to $O(\log \gamma)$ without

increasing the space complexity. So the total circuit depth is reduced to

$$O\left(\tau \log^2 \gamma \log^2 n\right). \quad (\text{S-39})$$

VI. SOLVING LINEAR SYSTEM

Ref. [35] developed an algorithm for solving linear system based on Hamiltonian simulation and state preparation, whose circuit depth is polynomial in $\log(1/\varepsilon)$. The result can be stated as

Lemma 5 (Theorem. 3 in [35]). *Let $|x\rangle$ be a quantum state proportional to $H^{-1}|b\rangle$. A quantum state $|\tilde{x}\rangle$ satisfying $\| |\tilde{x}\rangle - |x\rangle \| \leq \varepsilon$ can be output with $O\left(\kappa\sqrt{\log(\kappa/\varepsilon)}\right)$ uses of Hamiltonian simulation algorithm that approximates $e^{-i\hat{H}t}$ for $t = O(\kappa \log(\kappa/\varepsilon))$ with error $O\left(\varepsilon/\left(\kappa\sqrt{\log(\kappa/\varepsilon)}\right)\right)$, and $O\left(\kappa\sqrt{\log(\kappa/\varepsilon)}\right)$ queries of state preparation oracle \hat{B} satisfying $\hat{B}|0\rangle^{\otimes n} = |b\rangle$.*

We focus on the Hamiltonian in the form of Eq. (6) in the main text. Based on Lemma. 5, we have the following result.

Lemma 6. *Let \hat{H} be a Hermitian expressed as*

$$\hat{H} = \sum_{p=0}^{P-1} \alpha_p \hat{V}(p) \quad (\text{S-40})$$

with $\alpha_p > 0$, $\hat{V}(p) = \bigotimes_{i=0}^{n-1} \hat{V}_i(p)$, $\hat{V}_i(p) \in SU(2)$, and condition number κ . Let $|b\rangle$ be d -sparse quantum state. With only single- and two-qubit gates, the quantum state $|x\rangle$ proportional to $\hat{H}^{-1}|b\rangle$ can be approximately prepared to error ε using $\tilde{O}(\log(nP)\alpha\kappa^2 + \log(nd)\kappa)$ circuit depth and $O(n(P + d \log d))$ qubits, where \tilde{O} neglects the logarithmic dependence on $\kappa, 1/\varepsilon$.

Proof. According to Theorem. 3 for Hamiltonian simulation, for evolution time and error required by Lemma. 5, each Hamiltonian simulation has circuit depth $O(\log(nP)(\alpha\kappa \log(\kappa/\varepsilon) + \log((\kappa\sqrt{\log(\kappa/\varepsilon)})/\varepsilon)))$. So Hamiltonian simulation account for totally $\tilde{O}(\log(nP)\alpha\kappa^2)$ circuit depth, and $O(nP)$ ancillary qubits are required. According to Theorem. 2, for d -sparse $|b\rangle$, each query of the state preparation oracle \hat{B} has circuit depth $O(\log(nd))$, so the state preparation account for totally $\tilde{O}(\log(nd)\kappa)$ circuit depth, and $O(nd \log d)$ ancillary qubits are required. Combining the costs for Hamiltonian simulation and state preparation, Lemma. 6 can be obtained. \square

Theorem. 4 in the main text is achieved by setting $d = O(\text{poly}(n))$ for Lemma. 6. Moreover, by setting $P, \alpha, d = O(1)$, the circuit depth and qubit number reduce to $\tilde{O}(\log(n)\text{poly}(\kappa))$ and $O(n)$ respectively.

The comparison of our parallel method to other protocols for solving linear systems are provided in Table. S-I. Both quantum sequential and quantum parallel methods use the algorithm in [35] with the qubitization technique for Hamiltonian simulation [5], and the sparse state preparation method introduced in Theorem. 2. ‘‘Quantum sequential’’ corresponds to the method in [4, 33] for $\text{select}(\hat{V})$; ‘‘quantum parallel’’ corresponds to the method in Lemma. 1 for $\text{select}(\hat{V})$.

Supplementary Table S-I: Space and time complexities for SLS with $O(\text{poly}(n))$ -sparse $|b\rangle$. ‘‘ $O(1)$ -sparse’’ corresponds to $P, \alpha, d = O(1)$. We have defined $\kappa_F \equiv \|\hat{H}\|_F / \|\hat{H}\|$ with $\|\cdot\|_F$ the Frobenius norm.

Algorithm	Time	Space	Time ($O(1)$ -sparse)	Space ($O(1)$ -sparse)
Quantum-inspired [22, 23]	$\tilde{O}(\text{poly}(n, \kappa, \kappa_F))$	$O(nNP)$	$\tilde{O}(\text{poly}(n, \kappa, \kappa_F))$	$O(nN)$
Quantum sequential	$\tilde{O}(nP\alpha \text{poly}(\kappa))$	$O(\log P + \text{poly}(n))$	$\tilde{O}(n \text{poly}(\kappa))$	$O(n)$
Quantum parallel (this work)	$\tilde{O}(\log(nP)\alpha \text{poly}(\kappa))$	$O(P \text{poly}(n))$	$\tilde{O}(\log(n)\text{poly}(\kappa))$	$O(n)$

VII. GENERALIZED QRAM FOR CONTINUOUS AMPLITUDES

Originally, QRAM is designed for storing the classical binary data $\mathcal{D} = \{|D_k\rangle\}_{k=0}^{2^m-1}$ with $|D_k\rangle \in \{|0\rangle, |1\rangle\}$. Querying QRAM performs Eq. (7) in the main text:

$$\text{QRAM}(\mathcal{D}) \sum_{k=0}^{2^m-1} \psi_k |k\rangle |0\rangle = \sum_{k=0}^{2^m-1} \psi_k |k\rangle |D_k\rangle.$$

As noted in [39], QRAM can not be directly generalized to storing unknown quantum states with $|D_k\rangle \in \mathbb{C}^2$, due to the non-cloning theorem.

However, there are classical data with continuous values one may deal with, so the generalization of QRAM to continuous amplitude is still demanded. In other words, we want generalize the transformation in Eq. (7), with known, classical description of $|D_k\rangle \in \mathbb{C}^2$. A naive protocol is to digitize $|D_k\rangle$ [28, 41]. Let $|D_k\rangle = \alpha_k|0\rangle + \beta_k|1\rangle$ with complex values $|\alpha_k|^2 + |\beta_k|^2 = 1$, we define $|D_k\rangle'$ as an w -bit digital representation of α_k and β_k with error ε , which satisfies $w = O(\log(1/\varepsilon))$. We store each bit string $|D_k\rangle'$ in a memory cell. By querying the binary QRAM with m bus qubits, we are able to perform the transformation $|k\rangle|0\rangle^{\otimes w} \rightarrow |k\rangle|D_k\rangle'$. Introducing another qubit at state $|0\rangle$, implementing a rotation on it controlled by $|D_k\rangle'$, the transformation $|k\rangle|D_k\rangle'|0\rangle \rightarrow |k\rangle|D_k\rangle'|D_k\rangle$ can be obtained. Then, by querying the binary QRAMs again for uncomputation $|k\rangle|D_k\rangle'|D_k\rangle \rightarrow |k\rangle|0\rangle^{\otimes w}|D_k\rangle$, the target state is obtained. This process have circuit depth $O(mw) = O(m \log(1/\varepsilon))$ and requires $O(2^m + \log(1/\varepsilon))$ ancillary qubits.

On the other hand, with our PUM in Lemma. 1, the QRAM for continuous amplitudes can be realized much more efficiently. By setting $n = 1$, $|z\rangle = |0\rangle$ and

$$\hat{U}(k) = |0\rangle\langle D_k| + |1\rangle\langle D_k^\perp| \quad (\text{S-41})$$

with $\langle D_k|D_k^\perp\rangle = 0$, Eq. (S-21) is equivalent to Eq. (7) in the main text with $\tilde{n} = m$. According to Lemma. 1, it is straightforward to see that the circuit depth and ancillary qubits can be reduced to $O(m)$ and $O(2^m)$, which is independent of the precision ε .